
PERSONAL COMFORT ESTIMATION IN PARTIAL OBSERVABLE ENVIRONMENT USING REINFORCEMENT LEARNING

Shashi Suman¹, Ali Etemad¹, Francois Rivest²

¹Dept. ECE and Ingenuity Labs Research Institute, Queen's University

²Dept. of Mathematics and Computer Science, Royal Military College of Canada

{shashi.suman, ali.etemad}@queensu.ca, francois.rivest@{mail.mcgill.ca, rmc.ca}

ABSTRACT

The technology used in smart homes have improved to learn the user preferences from feedbacks in order to provide convenience to the user in the home environment. Most smart homes learn a uniform model to represent the thermal preference of user which generally fails when the pool of occupants includes people having different age, gender, and location. Having different thermal sensation for each user poses a challenge for the smart homes to learn a personalized preference for each occupant without forgetting the policy of others. A smart home with single optimal policy may fail to provide comfort when a new user with different preference is integrated in the home. In this paper, we propose POSHS, a Bayesian Reinforcement learning algorithm that can approximate the current occupant state in a partial observable environment using its thermal preference and then decide if its a new occupant or belongs to the pool of previously observed users. We then compare POSHS algorithm with an LSTM based algorithm to learn and estimate the current state of the occupant while also taking optimal actions to reduce the timesteps required to set the preferences. We perform these experiments with upto 5 simulated human models each based on hierarchical reinforcement learning. The results show that POSHS can approximate the current user state just from its temperature and humidity preference and also reduce the number of time-steps required to set optimal temperature and humidity by the human model in the presence of the smart home.

1 Introduction

1.1 Personalization In SmartHomes

With the current integration of machine learning, the adoption of smart homes is increasingly becoming popular. Devices such as smart thermostats are often limited to *personalized* schedules, which may not be ideal for multiple occupants with different thermal preferences, which in turn may lead to discomfort. Accordingly, the lack of complete environment information by the smart home may create uncomfortable scenarios for users (lack of personalization). In most cases, smart homes do not have the ability to identify occupants with varying preferences due to lack of ubiquitous biometric technologies in smart homes as well as privacy issues which can be encountered as a result of using sensing systems like cameras. The most common comfort parameter found in residences that smart homes have control over is temperature and humidity. In addition with smart watches and phones that can classify the activity of the user with a high accuracy [24], we believe that learning a personalized preference is possible.

1.2 Personalization using Machine Learning

Previously, smart home devices had profiles for each user where each user would integrate its daily routine for thermostat, humidifier, lights, etc. However these devices required manual entry whenever there is a change in the user. However, with the current advancement in machine learning, the personalization of users have improved by a vast amount. Studies such as [3, 8, 22] show that users' temperature and humidity can vary by 3°C and 12% respectively while these preference are also affected by age and gender. Having uniform thermal models across all user receive lower comfortable scores [3, 2]. So, we can conclude that the preference of users vary enough to be personalized. Recent

studies have explored into this and have began implementing machine learning algorithms such as Random Forests, Support Vector Machines, etc to learn the difference in the comfort preference of users [8, 9]. Parameters such as temperature, humidity, skin temperature, age, gender provide enough information for the algorithms to learn their preferences [17, 23]. Some studies that have utilized machine learning found many outliers that lie outside the range of average comfort level but receive more votes for being comfortable [2, 23].

1.3 Limitations of current methods

Even though the above algorithms are able to learn personal preferences, these model only work with data obtained from a fixed number of users and needs to be trained whenever a new user arrives but only after collecting data from the new user [17, 5, 11]. However, in a real scenario, we expect smart homes to quickly learn with the least amount of data available from the new user. Smart Homes such as [18] collects data during the day time and learn it during night. This brings a major limitation of the smart homes where it is expected for it to learn about a new user and improve the prediction in an online fashion or use transfer learning [1]. Another limitation with the above studies is that the algorithms need sufficient amount of parameters which may not be available in general homes like devices to measure skin sensation, ECG, EEG unless the user is wearing a smart watch. This leaves us with most commonly used comfort parameters like temperature and humidity. This poses a challenge as these parameters overlap withing multiple users.

1.4 How do we tackle the limitations ?

In this paper, we address this by improving our smart home model from our previous work [20] to take effective decisions when the current user is not explicitly observable using Reinforcement learning. This is possible through identification of users based on their detailed thermal preferences or learning the temporal relations between the sequence of actions taken for a given activity and TH. We simulate a series of experiments with an HRL-based human model from our previous work [20] capable of learning activities and setting its thermal preferences and an SHS that aims to learn its preferences. In this setup, the SHS agent does not have the complete information about the state of the environment (i.e. the occupant) and the SHS agent has to rely on the observation it receives at each time step. To accomplish the task of learning a policy with uncertainty, our agent maintains a belief over the human model that is pursuing its activity in the environment. Our experiments show that the SHS can learn to accurately identify the current user in the environment based on its thermal preferences given the current activity. Beyond identifying the occupant in the environment, SHS also learns the thermal preference of each activity of each identified user which can be used for further personalization.

In the next section, we describe the architecture of the smart home agent that can *a)* learn to recognize the current user and to set the TH according to its preferences, and *b)* learn the temporal relation between the embedding of the sequence of thermal preferences for multiple users. We then compare the performance of each agent for two to five human occupants. Finally, we discuss the limitation of each SHS agent and where they fail to learn the preferences. Our results show that the smart home can accurately identify the user based on their thermal preferences with high accuracies. We run our experiments with small and moderate differences in metabolism rate and observe that models with similar thermal preferences lowers the accuracy in prediction but does not increase the time-steps required to set the temperature and humidity settings by the human model.

2 Related Work

In this section, we review some papers that have explored into personalization of user’s thermal comfort by predicting the thermal sensation of the user and then taking optimal action. We review some research work that explore into personalized thermal preference of the occupants and using machine learning algorithms to predict the thermal sensation of the users.

Occupant Personalization With multiple users in a home having different thermal preferences, smart homes need to have a personalized profile for each occupant. For instance, in [8], boosted trees were used to learn occupant’s personalized thermal responses using skin temperature and its surrounding with median accuracy of 0.84. Similarly, in [9], occupants heating and cooling behaviors were used to design personalized comfort models with a prediction accuracy of 0.73. Authors in [7] show that human occupants have different thermal perceptions in indoor environments based on heat exchange through skin and achieved a median accuracy of 85% for classifying thermal preferences with humans in the loop. In [25], authors implemented Support Vector Machine to learn and classify the individual occupant’s thermal sensation indoors with an accuracy of upto 86%. Experiments in [3] show that on an average, the thermal sensation of humans have a standard deviation of 3°C. This can also be confirmed from [17] where thermal sensation of fixed number of users showed that different users perceive the same surroundings in a different way thus can

be used to personalize. The parameters used in [17] were electrodermal activity, humidity, operational skin temperature, and heart rate to classify the users using Support Vector Machine. Similarly in [11], authors were able to reduce the thermal prediction of fixed users by 50% using Support Vector Machines. The mentioned works use sophisticated sensors attached to the body to obtain a personalized data about the user. However, factors such as age, gender also play role in thermal perception. [5] included age and outside temperature in the model of [3] to obtained a personalized comfort on fixed number of occupants and obtained a prediction accuracy of 76.7% using Support Vector Machines. Similarly, [22] included the parameter of gender to estimate the comfort of individuals. The mentioned research works converge on a common aim of suggesting that "one-model-fit" cannot work with all individuals. This cannot fit all. [23] explored this in details and found many outliers in the thermal votes that did not fit the basic thermal model of [3] using k -Nearest Neighbour. After including these outliers, the thermal sensation among the occupants improved significantly. Similarly, in [13], authors discovered that nearly 30% of the users showed discomfort when placed within same thermal conditions. To implement a personalized preference model, authors in [13] used Random Forest models and obtained a mean accuracy of 75% to predict personalized thermal parameters.

These studies imply that a personal model is necessary to learn the optimal comfort the user in the home. These studies have however focused more on fixed number of individuals with sophisticated sensors to measure skin temperature, heart rate, cardiac rhythm, etc. This involves offline learning by ML and RL algorithms and cannot accommodate users on the run in the home.

In the next section, we will discuss about a model of smart home that can learn about new occupants in an online fashion to personalize the comfort using common available parameters like temperature, humidity.

3 Methods

In this section, we extend the RL-based SHS system from our previous work [20] with the ability to estimate who is the current occupant using current TH and the human model's activity and actions only. The assumption for this problem is that there is only one human model in the environment at a given time. In this section, we first describe the general framework for the problem. Next, we will describe our proposed solution. Finally we will describe an alternate (baseline) solution.

3.1 Partial Observable Markov Decision Process

When there is uncertainty about the current state state of the environment (in this case, who the current occupant is, or what its preference are), a common framework for RL is the Partial Observable Markov Decision Process (POMDP) [15, 16, 6, 26]. A POMDP is defined by the tuple $\langle \mathcal{S}, \mathcal{A}, \Omega, T, R, O, \gamma, b_0 \rangle$, where \mathcal{S} is the set of discretized states, \mathcal{A} is the set of actions, and Ω is the set of observations. Moreover, $T(s_t, a_t, s_{t+1}) : [\mathcal{S} \times \mathcal{A} \times \mathcal{S}] \rightarrow [0, 1]$ is the transition function that defines the probability of ending in state s_{t+1} after taking action a_t in state s_t , R is the reward function that specifies the immediate reward received after taking action a in state s_t , and $O(a_t, o_{t+1}, s_{t+1}) : [\mathcal{A} \times \Omega \times \mathcal{S}] \rightarrow [0, 1]$ is the observation function that defines the probability of observing o_{t+1} after taking action a_t and ending in state s_{t+1} . Lastly, γ is the discount factor and b_0 is the initial belief state that defines a probability over the observable state of the environment.

To calculate the belief about the current state, POMDP uses the Bayes theorem, which is defined as:

$$P(A|B) = \frac{P(B|A)P(A)}{P(B)}, \quad (1)$$

where A and B are the events, $P(A)$ is the prior, $P(B)$ is the evidence, $P(A|B)$ is the posterior probability of event A given that event B has occurred, $P(B|A)$ is the probability of event B given that event A has occurred (likelihood). Here, we set A as a possible human model \mathcal{H}_i in the home, and B as the next TH and activity o_{t+1} observed by the smart home. Note that here the state is the concatenation of the observation o_{t+1} and the current occupant \mathcal{H}_i ($s_t = [o_t, \mathcal{H}_i]$), but the belief only needs to be over the occupants (since the TH and activity are fully observable). Accordingly, $P(B|A)$ is the probability of observing TH preferences given user \mathcal{H}_i from the observation function O . $P(A|B)$ is the posterior probability of the human occupant \mathcal{H}_i given the current activity and TH of the environment and previous belief. Finally $P(A)$ is the prior probability of human occupant \mathcal{H}_i derived from the transition function T , while $P(B)$ is the marginal probability of the current observation received from the environment. Given our problem setup, the smart home agent takes an action a_t at every time-step after which it receives an observation o_{t+1} (consisting of the current activity of the occupant, temperature, and humidity) from the environment. With this observation, a

POMDP agent would update its belief over each possible occupant by the following equation:

$$\underbrace{b_{t+1}(\mathcal{H}_i)}_{P(A|B)} = \frac{\underbrace{O(a_t, o_{t+1}, [o_{t+1}, \mathcal{H}_i])}_{P(B|A)} \sum_{\mathcal{H}_j \in \mathcal{H}} \underbrace{T([o_t, \mathcal{H}_j], a_t, s_{t+1}) b_t(\mathcal{H}_j)}_{P(A)}}{\underbrace{Pr(o_{t+1}|b_t, a_t)}_{P(B)}}, \quad (2)$$

where $b_t(\mathcal{H}_i)$ is the previous belief (probability) that the occupant is human model \mathcal{H}_i , $b_{t+1}(\mathcal{H}_i)$ is the updated belief for the next time step, and $Pr(o_{t+1}|b_t, a_t)$ is the probability of observing o_{t+1} when action a_t is taken with the belief vector b_t over all possible human models (or occupants) \mathcal{H} . The denominator is given by:

$$\begin{aligned} Pr(o_{t+1}|b_t, a_t) &= \sum_{\mathcal{H}_k \in \mathcal{H}} O(a_t, o_{t+1}, [o_{t+1}, \mathcal{H}_k]) \\ &\times \sum_{\mathcal{H}_j \in \mathcal{H}} T([o_t, \mathcal{H}_j], a_t, s_{t+1}) b_t(\mathcal{H}_j). \end{aligned} \quad (3)$$

It should be noted that in the context of our problem, the transition function T and observation function O are unknown. Therefore, in the next sections we will describe our solution around this issue.

3.2 Partial Observable Smart Home System

Here, we describe a modified SHS that implements a Bayesian model to learn multiple user's personalized TH preferences when the user information is limited. Accordingly, we define a Partial Observable Smart Home System (POSHS) as a Bayesian model [15, 16] of the SHS where the state of the environment is not fully observable as discussed in the previous section. We will further assume that the model of the occupant does not change during an episode (a set of 3 activities). We will then use the Bayes theorem and the learnt occupants' TH preferences to infer the current human model in the environment, thus identifying it.

We depict an overview of POSHS in Figure 1, where it is divided into two components (panels (a) and (b)). During the episode (panel (a)), at each time step, the agent estimates a probability distribution over the TH preferences of the current occupant based on the TH and activity observations. This distribution is combined with a pool of previously learned user TH preference distributions using the Bayes theorem to estimate the belief state over the possible current occupants. The belief state is then used to weight the Q -table of each possible occupant in order to select the optimal action for the current belief. At the end of the episode (panel (b)), the agent compares the final estimated TH preference distribution to the pool of learned preferences. If a match is found, then the episode distribution parameters are used to update that occupant's TH preference distribution. If a match is not found, we assume this is a new user. Therefore, the estimated probability TH preference distribution is added to the pool along with a new Q -table. Finally, the Q -tables are updated with the episode data. In the next subsections, we describe these elements (TH preference distribution, belief estimation, distribution similarity, and Q update) in depth.

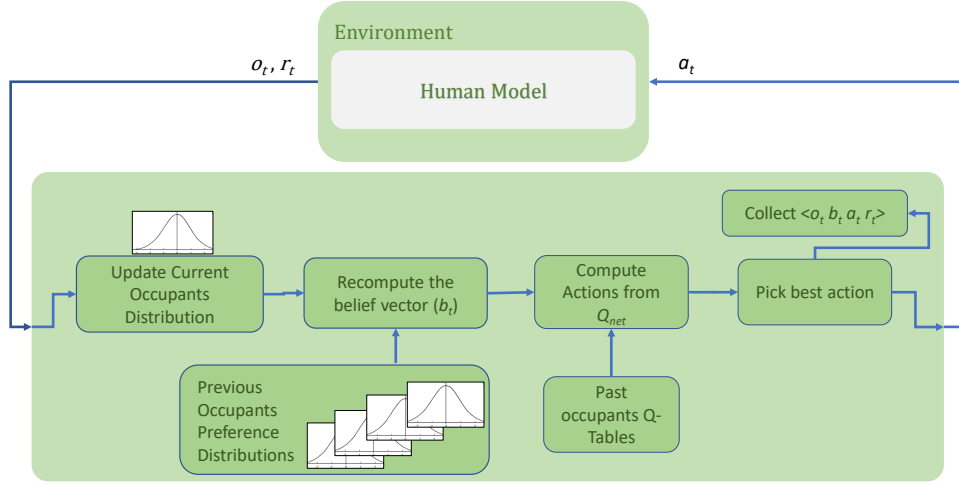
3.3 TH Preference Distribution

Since it is impossible to fully define T and O for an unknown set of occupants, we need a different approach to estimate the SHS belief over the set of possible occupants during the episode. To make the problem more tractable, we first assume that the occupants are the same through the whole episode. This implies that the transitional probabilities in an episode have the following property:

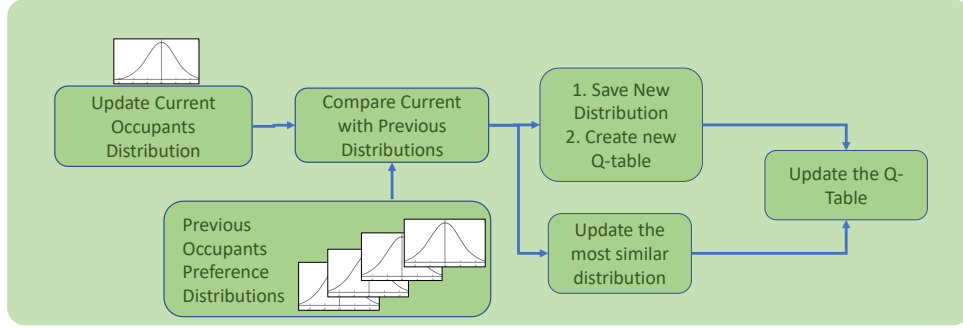
$$\begin{aligned} T([o_t, \mathcal{H}_i], a_t, [o_{t+1}, \mathcal{H}_j]) &= 0 \quad \forall i \neq j \\ T([o_t, \mathcal{H}_i], a_t, [o_{t+1}, \mathcal{H}_i]) &= 1. \end{aligned} \quad (4)$$

Accordingly, given a potential occupant \mathcal{H}_i , we need to define a probability distribution over the TH preference for each activity ($P(B|A)$ in Eq. 2). Using the Bayes rule, this will provide a way to estimate the probability of a specific occupant, given the TH observation ($P(A|B)$ in Eq. 2). The TH preference probability distribution $P(TH|\mathcal{H}_i)$ of a given occupant \mathcal{H}_i over temperature and humidity for each activity is described by a Gaussian distribution given as:

$$P(TH|\mathcal{H}_i) = \frac{1}{\sigma_t \sqrt{2\pi}} \exp \left(-\frac{1}{2} \left(\frac{TH - \mu_{\mathcal{H}_i}}{\sigma_{\mathcal{H}_i}} \right)^2 \right), \quad (5)$$



(a) POSHS during the episode



(b) POSHS at the end of episode

Figure 1: (A) POSHS during the episode: belief is computed and action is taken based on the current belief vector. The observation transitions are stored and distribution parameters are updated. (b) POSHS at the end of the episode: the current observed distribution is compared with stored distributions. If the distance between the distributions is greater than a threshold, a new Q -table is created for the new human occupant, otherwise the parameters of the distribution most similar to the current distribution are updated.

where TH is an observed temperature (or humidity) and $\mu_{\mathcal{H}_i}$ and $\sigma_{\mathcal{H}_i}$ are the mean and standard deviations of the of the preference distribution for occupant \mathcal{H}_i . The above equation is defined individually for both temperature and humidity, and for each activity.

Given a complete episode, the SHS samples each observation when the human agent is not making any changes to the TH and continues with a given activity. Accordingly, the parameters of the TH preference distribution for the occupant of that episode can be estimated using best point estimators given by

$$\mu_e = \frac{1}{C} \sum_{\text{valid } t=0}^T TH_t \quad (6)$$

and

$$\sigma_e = \sqrt{\frac{1}{C} \sum_{i=0}^T (TH_i - \mu_t)^2}, \quad (7)$$

where TH_t is the observed temperature or humidity at time step t for the given activity, C is the number of valid observations, and T is the length of the episode. Therefore, a complete TH preference probability distribution for a model can be coded using a 12D vector ($2 \text{ parameters} \times 2 \text{ TH} \times 3$).

3.4 Belief Estimation

Here, we describe the mathematical formulation of the belief estimation of the smart home about the human occupant at time step t given observation TH_t . For simplicity, let us assume that we have two human agents in a given smart home environment denoted by \mathcal{H}_a and \mathcal{H}_b . Restructuring Eq. 2 for human model \mathcal{H}_a and \mathcal{H}_b based on the Bayes theorem, we obtain:

$$\frac{P(TH_t|\mathcal{H}_a)}{P(TH_t|\mathcal{H}_b)} = \frac{P(\mathcal{H}_a|TH_t)P(\mathcal{H}_b)}{P(\mathcal{H}_b|TH_t)P(\mathcal{H}_a)}. \quad (8)$$

Solving the above equation for \mathcal{H}_a and \mathcal{H}_b , we obtain:

$$P(\mathcal{H}_a|TH_t) = \frac{P(TH_t|\mathcal{H}_a)P(\mathcal{H}_a)}{P(TH_t|\mathcal{H}_a)P(\mathcal{H}_a) + P(TH_t|\mathcal{H}_b)P(\mathcal{H}_b)} \quad (9)$$

and

$$P(\mathcal{H}_b|TH_t) = \frac{P(TH_t|\mathcal{H}_b)P(\mathcal{H}_b)}{P(TH_t|\mathcal{H}_a)P(\mathcal{H}_a) + P(TH_t|\mathcal{H}_b)P(\mathcal{H}_b)}. \quad (10)$$

Given N different human models, we can define the probability of the i^{th} human model \mathcal{H}_i at the t_{th} time-step as:

$$P(\mathcal{H}_i|TH_t) = \frac{P(TH_t|\mathcal{H}_i)P(\mathcal{H}_i)}{\sum_{i=0}^N P(TH_t|\mathcal{H}_i)P(\mathcal{H}_i)}. \quad (11)$$

Dividing $P(\mathcal{H}_a|TH_t)$ by $P(\mathcal{H}_b|TH_t)$ from Eq. 9 and Eq. 10, and then substituting $P(TH_t|\mathcal{H})$ with Eq. 5 we obtain:

$$\begin{aligned} \frac{P(\mathcal{H}_a|TH_t)}{P(\mathcal{H}_b|TH_t)} &= \frac{\frac{1}{\sigma_{\mathcal{H}_a}\sqrt{2\pi}} \exp\left(-\frac{1}{2}\left(\frac{TH_t - \mu_{\mathcal{H}_a}}{\sigma_{\mathcal{H}_a}}\right)^2\right) P(\mathcal{H}_a)}{\frac{1}{\sigma_{\mathcal{H}_b}\sqrt{2\pi}} \exp\left(-\frac{1}{2}\left(\frac{TH_t - \mu_{\mathcal{H}_b}}{\sigma_{\mathcal{H}_b}}\right)^2\right) P(\mathcal{H}_b)} \\ &= \frac{\sigma_{\mathcal{H}_b}}{\sigma_{\mathcal{H}_a}} \frac{\exp\frac{1}{2}\left(\left(\frac{TH_t - \mu_{\mathcal{H}_a}}{\sigma_{\mathcal{H}_a}}\right)^2 - \left(\frac{TH_t - \mu_{\mathcal{H}_b}}{\sigma_{\mathcal{H}_b}}\right)^2\right) P(\mathcal{H}_a)}{P(\mathcal{H}_b)}. \end{aligned} \quad (12)$$

Assuming $\sigma_{\mathcal{H}_a} \approx \sigma_{\mathcal{H}_b} = \sigma$, we get:

$$\frac{P(\mathcal{H}_a|TH_t)}{P(\mathcal{H}_b|TH_t)} = \frac{\exp\frac{1}{2\sigma^2}((2TH_t - \mu_{\mathcal{H}_a} - \mu_{\mathcal{H}_b}))}{\frac{P(\mathcal{H}_b)}{(\mu_{\mathcal{H}_a} - \mu_{\mathcal{H}_b})P(\mathcal{H}_a)}}. \quad (13)$$

At the beginning of the training episode, the POSHS agent has no information about the user, thus maintains an equal initial belief for each possible human occupant. Accordingly, the prior probability of each model can be defined as $P(\mathcal{H}_a) = P(\mathcal{H}_b)$. Hence, we can rewrite Eq. 13 as

$$\begin{aligned} \frac{P(\mathcal{H}_a|TH)}{P(\mathcal{H}_b|TH)} + 1 &= \frac{P(\mathcal{H}_a|TH) + P(\mathcal{H}_b|TH)}{P(\mathcal{H}_b|TH)} = \frac{1}{P(\mathcal{H}_b|TH)} \\ &= \exp\frac{1}{2\sigma^2}((2TH_t - \mu_{\mathcal{H}_a} - \mu_{\mathcal{H}_b})(\mu_{\mathcal{H}_a} - \mu_{\mathcal{H}_b})) + 1. \end{aligned} \quad (14)$$

This gives

$$P(\mathcal{H}_b|TH) = \frac{1}{\exp\frac{1}{2\sigma^2}((2TH_t - \mu_{\mathcal{H}_a} - \mu_{\mathcal{H}_b})(\mu_{\mathcal{H}_a} - \mu_{\mathcal{H}_b})) + 1} \quad (15)$$

and

$$P(\mathcal{H}_a|TH_t) = \frac{\exp\frac{1}{2\sigma^2}((2TH_t - \mu_{\mathcal{H}_a} - \mu_{\mathcal{H}_b})(\mu_{\mathcal{H}_a} - \mu_{\mathcal{H}_b}))}{\exp\frac{1}{2\sigma^2}((2TH_t - \mu_{\mathcal{H}_a} - \mu_{\mathcal{H}_b})(\mu_{\mathcal{H}_a} - \mu_{\mathcal{H}_b})) + 1}. \quad (16)$$

With the above equation, we derive the *initial* posterior for each human agent at each time step for two human occupants. At the next time step we perform the Bayesian update where the posterior ($P(\mathcal{H}_i|HT_t)$) at time step t becomes the prior ($P(\mathcal{H}_i)$) at time step $t + 1$. Accordingly, we can take Eq. 8 and divide both numerator and denominator by the $P(TH_t|\mathcal{H}_a)$, and then replace the ratio in the second term of the denominator by Eq. 12. This yields:

$$\begin{aligned} P(\mathcal{H}_a|TH_t) &= \frac{P(TH_t|\mathcal{H}_a)P(\mathcal{H}_a)}{P(TH_t|\mathcal{H}_a)P(\mathcal{H}_a) + P(TH_t|\mathcal{H}_b)P(\mathcal{H}_b)} \\ &= \frac{P(\mathcal{H}_a)}{P(\mathcal{H}_a) + \frac{P(TH_t|\mathcal{H}_b)}{P(TH_t|\mathcal{H}_a)}P(\mathcal{H}_b)} \\ &= \frac{P(\mathcal{H}_a)}{P(\mathcal{H}_a) + C(\mathcal{H}_b, \mathcal{H}_a)P(\mathcal{H}_b)}. \end{aligned} \quad (17)$$

where

$$C(\mathcal{H}_b, \mathcal{H}_a) = \exp \left(\frac{(2TH_t - \mu_{\mathcal{H}_b} - \mu_{\mathcal{H}_a})(\mu_{\mathcal{H}_b} - \mu_{\mathcal{H}_a})}{2\sigma^2} \right). \quad (18)$$

Similarly, for Model \mathcal{H}_b , the posterior can be computed as:

$$P(\mathcal{H}_b|TH) = \frac{P(\mathcal{H}_b)}{C(\mathcal{H}_a, \mathcal{H}_b)P(\mathcal{H}_a) + P(\mathcal{H}_b)}. \quad (19)$$

Expanding the above equations for N human models, we can get our posterior for the i^{th} human model as:

$$P(\mathcal{H}_i|TH_i) = \frac{P(\mathcal{H}_i)}{\sum_{j=0}^N C(\mathcal{H}_j, \mathcal{H}_i)P(\mathcal{H}_j)}, \quad (20)$$

3.5 Distribution Similarity

Upon completion of an episode, the SHS agent needs to know if the current occupant belongs to the pool of previously observed occupants or if it is a new occupant in the environment. To do so, the SHS agent follows the procedure in Figure 1(b). Here, the best point estimators (μ_e and σ_e from Eqs. 6 and 7) for the current occupant TH distribution are computed. The resulting TH preference distribution is then compared with the distributions in the pool of previously observed occupants using the Jensen-Shannon Divergence (JSD) measure [4]. We select this particular divergence measurement since it has shown success in similar RL-related applications in prior works [19]. Moreover, this metric provides benefits over other divergence metrics, in particular, (a) when variations between distributions are small, the divergence remains smooth, and (b) the divergence between distributions is symmetric, i.e., $JSD(P_0, P_1) = JSD(P_1, P_0)$.

The Jensen-Shannon divergence between n probability distributions is formulated as:

$$JSD = H \left[\sum_{i=1}^n w_i p_i \right] - \sum_{i=1}^n w_i H(p_i), \quad (21)$$

where H is the Shannon entropy [12] and w_i are the weights selected for each probability distribution p_i . For our problem, we compare only two distributions at an instance, i.e., the current distribution of the occupant in question and each of the distributions from the pool of observed occupants. As a result, we set $n = 2$, and thus $w_1 = w_2 = 0.5$. Next, we define a new term τ_{JSD} as the threshold such that

$$JSD \geq \tau_{JSD} \iff \text{Different Human Model}, \quad (22)$$

where JSD is the measured Jensen-Shannon divergence between the two TH distributions. If the divergence between the distributions is greater than τ_{JSD} , the current occupant's distribution is added to the pool and the SHS agent creates a new Q -table. Otherwise the distribution with the smallest divergence (distribution with highest likelihood) is updated using a moving average with the current estimated parameters to improve the long term estimation of the occupant's preference distribution.

3.6 Q Update

Here, we describe the computation of the Q values of state-action pairs for a given occupant, followed by optimally selecting the best action using the belief vector over the user space. During each episode as shown in Figure 1(a), the SHS agent updates the TH distribution estimation parameters. It then calculates the belief vector using Bayes rule after which the Q -tables of the observed occupants are weighted using their belief vector to get a summarized Q_{net} value. The SHS agent then chooses the optimal action from the Q_{net} values of all the possible actions, which is then executed in the environment. The observation o_t , computed belief b_t , action taken a_t , and the reward received r_{t+1} from the environment are all stored in the memory.

To calculate the weighted Q update, each weight is decided by the belief of the specific human model for a given state from the belief vector. This update is given by the following equation:

$$Q_{net}(o_t, a_t) = \sum_{\mathcal{H}} b_t(\mathcal{H}) Q_{\mathcal{H}}(o_t, a_t), \quad (23)$$

where o_t is the observation, a_t is the chosen action, the weight $b_t(\mathcal{H}) = P(\mathcal{H}|TH_t)$ is the conditional probability given the current TH , and Q_{net} is the weighted sum of all Q values of all the occupants for a given observation.

Accordingly, we now update the Q table for a given occupant \mathcal{H} . Let b_t be the belief vector at time step t in the episode and $b_t(\mathcal{H})$ be the belief component of b_t for human \mathcal{H} . Moreover, let o_t be the received observation at time step t in the episode, $\alpha = 0.05$ be the learning rate, $\gamma = 0.98$ be the discount factor, and r_{t+1} be the reward received after action a_t from observation o_t at time step t . Accordingly, the $Q_{\mathcal{H}}$ update is given by

$$Q_{\mathcal{H}}(o_t, a_t) = (1 - \alpha)Q_{\mathcal{H}}(o_t, a_t) + \alpha[r_{t+1} * b_t(\mathcal{H}) + \gamma \max_{a'} Q_{\mathcal{H}}(o_{t+1}, a')]. \quad (24)$$

With the updated Q_{net} value, the agent can select the optimal action. For a given observation o_t , actions are selected using a decaying ϵ -Greedy policy keeping a balance between exploration and exploitation. The policy is given by:

$$\pi(o_t) = \begin{cases} \arg \max_{a \in \mathcal{A}} \{Q_{net}(o_t, a)\} & \text{with probability } 1 - \epsilon \\ a \in \mathcal{A} & \text{with probability } \epsilon/|\mathcal{A}| \end{cases}, \quad (25)$$

where ϵ is a threshold value between 0 and 1, and \mathcal{A} is the set of all possible actions.

3.7 Pseudocodes

In order to better facilitate reproduction of our work, in this subsection we present the pseudocodes and detailed algorithms for computing the Jensen-Shanon divergence, action selection and belief estimation, Q table update, and POSHS, in Algorithms 1 through 4.

Algorithm 1 Jensen-Shannon Divergence

```

1: function JSD(Distribution  $d_a$ , Distribution  $d_b$ , Amplification Factor  $A_f$ )
2:   let  $d_c = \frac{d_a + d_b}{2}$ 
3:   let  $H_a = d_a \times \log \frac{d_a}{d_c}$  ▷ Calculate Shannon entropy for  $d_a$ 
4:   let  $H_b = d_b \times \log \frac{d_b}{d_c}$  ▷ Calculate Shannon entropy for  $d_b$ 
5:    $\tau = \sqrt{\frac{\sum H_a + \sum H_b}{2}}$ 
6:   return  $A_f * \tau$ 

```

Algorithm 2 GetAction

```

1: function GETACTION( $o_t$ )
2:   let  $N$  = number of human models
3:   let  $TH_t \leftarrow o_t$ 
4:   calculate belief  $P(\mathcal{H}_i | TH_t) = \frac{P(TH_t | \mathcal{H}_i)P(\mathcal{H}_i)}{\sum_{i=0}^N P(TH_t | \mathcal{H}_i)P(\mathcal{H}_i)}$  ▷ Belief update
5:    $Q_{net}(o_t, a_t) = P(\mathcal{H}_a)Q_a(o_t, a_t) + P(\mathcal{H}_b)Q_b(o_t, a_t) + \dots + P(\mathcal{H}_n)Q_n(o_t, a_t)$ 
6:   return  $\arg \max_a Q(o_t, a)$ 

```

Algorithm 3 Update

```

1: function UPDATE( $memory$ ,  $newNode$ )
2:   let  $N$  = number of human models
3:   for  $\mathcal{H}$  in all human models do
4:     let  $b = P(\mathcal{H})$  ▷ Belief  $i_{th}$  human model
5:     if  $newNode$  then
6:        $Q_{\mathcal{H}} \leftarrow 0$  ▷ initialize  $Q$  table for unobserved human model
7:     Endif
8:     for  $\langle o_t, a_t, o_{t+1}, r_{t+1} \rangle$  in  $memory$  do
9:        $Q_{\mathcal{H}}(o_t, a_t) = (1 - \alpha)Q_{\mathcal{H}}(o_t, a_t) + \alpha[r_{t+1} * b + \gamma \max_{a'} Q_{\mathcal{H}}(o_{t+1}, a')]$ 
10:    Endfor
11:  Endfor

```

Algorithm 4 Partially Observable Smart Home System (POSHS)

```
1: let  $\mu_{TH} = \{ \}$  ▷ Set containing Model's mean TH
2: let  $\sigma_{TH} = \{ \}$  ▷ Set containing Model's deviation of TH
3: let  $Q_{\mathcal{H}} = \{ \}$  ▷ Set containing Model's Q Table
4: let  $o_0 = \mathcal{O}(s_0)$  where  $o_t$  is partial observation of state  $s_t$ 
5: for each  $e$  in episodes do
6:   let  $C = 0$ 
7:   let  $\mu_e = 0$  ▷ Current Episode mean of TH
8:   let  $\sigma_e = 0$  ▷ Current Episode standard deviation of TH
9:   let memory = [ ]
10:  while  $o_t$  is not terminal do
11:    with greedy policy  $a_t = \text{getAction}(o_t)$  ▷ Algorithm 2
12:    execute  $a_t$ 
13:    observe  $o_{t+1}, r_{t+1}$ 
14:    update  $\mu_e, \sigma_e$  for  $C$  time-steps
15:    append  $\langle o_t, a_t, o_{t+1}, r_{t+1} \rangle$  in memory
16:     $C = C + 1$ 
17:  Endwhile
18:  let newNode = False ▷ Flag to indicate a new human user
19:  let divergence = [ ]
20:  for  $\langle \mu, \sigma \rangle$  in  $\mu_{TH}, \sigma_{TH}$  do
21:    let  $d_a = \text{PDF}(\mu_e, \sigma_e)$ 
22:    let  $d_b = \text{PDF}(\mu, \sigma)$ 
23:    let  $k = \text{JSD}(d_a, d_b)$  ▷ Algorithm 1
24:    append  $k$  in divergence
25:  Endfor
26:  if  $\min(\text{distance}) > \tau_{JSD}$  & newNode then
27:    add  $\mu_e, \sigma_e$  in  $\mu_{TH}, \sigma_{TH}$  ▷ Add New Human Node
28:    newNode = True
29:  else if newNode then
30:    let  $i = \arg \min(\text{divergence})$ 
31:    let  $m = 0.5$  ▷ Moving filter significance
32:     $\mu_{TH}[i] = (1 - m)\mu_e + m\mu_{TH}[i]$ 
33:     $\sigma_{TH}[i] = (1 - m)\sigma_e + m\sigma_{TH}[i]$ 
34:  Endif
35:  update(memory, newNode) ▷ Algorithm 3
36: Endfor
```

4 Baseline

In this section, we describe a baseline method that we design and implement with which to compare our proposed method (POSHS) against. This baseline includes a Recurrent Neural Network (RNN) that can remember sequences of TH preferences in order to solve a partial observable environment. Classical RNNs, however, often suffer from issues such as vanishing gradient, making it difficult for the model to remember long-term information. As a result, we use a Long Short-Term Memory (LSTM) networks as our baseline. LSTM is a type of RNN that can hold a sequence of information in its memory and learn temporal relations. To do this, LSTM uses long-term sequences in memory referred to as ‘cell-state’. The output from previous time-steps are referred to as ‘hidden-state’. Information in an LSTM is controlled via three gates given as (a) forget-gate, which decides the information that needs to be rejected or accepted, (b) input-gate, which is used to control the information into the cell-state, and (c) output-gate, which generates the output for each time-step.

In a POMDP environment, Deep Q Network (DQN) fails to learn the optimal policy because it assume complete information about the state which we lack in our problem. Unlike DQNs, LSTM networks are capable of remembering long sequences of TH preferences and encoding the observation onto a latent space vector, making it possible to approximate the underlying hidden state [6, 26]. Thus, unlike POSHS where the agent needs to recognize the hidden state of the human occupant using Bayes rule explicitly, LSTMs can implicitly learn the underlying states using its recurrent memory.

To use LSTM as a baseline, we design two networks namely *train* and *target*. Both networks have the same architecture and are initialized with the same weights and biases. The inputs are sequences of TH, activity, and human action of the occupant. The input layer of the model is a 1D convolutional layer with 32 filters, a kernel size of 1, a stride of 1, and a Rectified Linear Unit (ReLU) activation function. The output of this layer is fed to an LSTM layer with 175 cells followed by a tanh activation function. In the end, the output of this layer is fed to a dense layer of 5 neurons and ReLU activation to output the Q -values for each possible action (total of 5 actions: increase/decrease T and H, and no action). The training procedure for this baseline is described in detail in Algorithm 5 with its architecture shown in Figure 2.

Algorithm 5 Deep Recurrent Q-Learning for POMDP Environment

```

1: Initialize train = train network with weights  $\theta$ 
2: Initialize target = target network with initial weights  $\theta^- = \theta$ 
3: let stateMemory = [ ]
4: let  $C = 0$ 
5: let  $o_t = \mathcal{O}(s_t)$  where  $o_t$  is partial observation of state  $s_t$  at time step  $t$ 
6: while  $i < \text{episodes}$  do
7:   while  $o_t$  is not terminal do
8:     with probability  $\epsilon$  select random action
9:     else select  $a_t = \arg \max_a Q_t(o_t, h_{t-1}, a | \theta)$ 
10:    execute  $a_t$ 
11:    observe  $o_{t+1}, r_t$ 
12:    Store the transition  $\langle o_t, a_t, o_{t+1}, r_t \rangle$  in stateMemory
13:     $C = C + 1$ 
14:  Endwhile
15:  for  $\langle o_t, a_t, o_{t+1}, r_t \rangle$  in stateMemory do
16:     $Q_t \leftarrow \text{Predict } Q | \theta \text{ for } o_{t+1} \text{ from } \textit{train}$ 
17:     $Q^- \leftarrow \text{Predict } Q | \theta^- \text{ for } s_{t+1} \text{ from } \textit{target}$ 
18:     $Q_{\max_{t+1}}^- = \max Q^-$ 
19:    if  $o_{t+1}$  is terminal then
20:       $y_t \leftarrow r_t$ 
21:    else
22:       $y_t \leftarrow r_t + \gamma Q_{\max_{t+1}}^-$ 
23:    Endif
24:    calculate loss  $\mathcal{L} = (y_t - Q_t)^2$ 
25:  Endfor
26:  fit train
27:  After  $C$  steps  $\theta^- \leftarrow \theta$ 
28: Endwhile

```

In this algorithm, in contrast to POSHS where we update the Q -values directly, we update the parameters of the network with which we predict the next Q -value. The Q -values of the current state from the *train* network are updated using the Q -values of the next state from the *target* network. Using the same network (*train*) for predicting the target Q -value would cause instability in the target Q -value. The weights for the *train* and *target* networks are represented by θ and θ^- respectively. Target weights θ^- are updated after every C iterations with θ , where C is a hyper-parameter set to 7 empirically. We use MSE as our loss function and ADAM [10] optimizer. We define our loss function similar to the update in table-based Q -learning which is the difference between the target and current Q -values. Accordingly, the loss function is given by

$$\mathcal{L}(s_t, a_t | \theta) = (r_t + \gamma \max_a Q(s_{t+1}, a | \theta^-) - Q(s_t, a_t | \theta))^2. \quad (26)$$

4.1 User Recognition

In order to recognize the user, the LSTM model uses the embedding of the sequence of TH preferences. However, for this embedding, the input sequence contains preferences of the occupant when it is **not** making any changes in TH which means that we only select TH preferences when the occupant is either executing the *continue* or *leave* action in a given activity. The embedding is obtained from the hidden state of the last cell from the LSTM layer of the architecture (Figure 2).

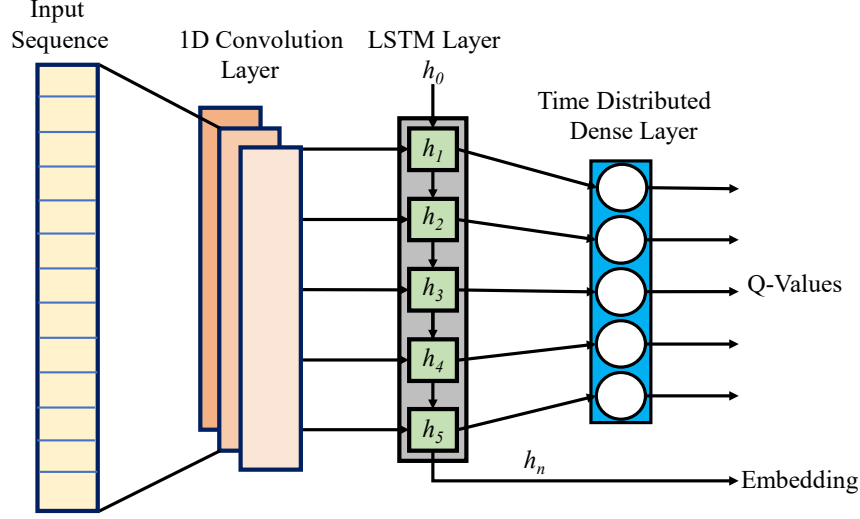


Figure 2: LSTM architecture: Input is a variable length sequence with 5d features which is convoluted in 1-dimension. The convoluted outputs is fed to the LSTM layer which is connected with a Time distributed dense layer outputting five Q -values for five actions to be taken by the SHS.

Before training, the initialized weight of the LSTM layer is same irrespective of the number of occupants. This helps the model to ensure that different embeddings are obtained for different TH sequences. The embedded information of TH sequence is collected at the end of episode when the model converges. At the end of episode, the obtained embedding is compared with each embedding stored in the pool. To compare the embedding, we use Kolmogorov Smirnov Test (KST) [14]. This test quantifies the distance between two empirical distributions and returns the p -value with which we can accept or reject the null hypothesis. For our problem, the null hypothesis is that two distributions are same. The equation to compute KST for two empirical distributions F_a and F_b (of the embeddings of TH sequence) is given as:

$$D = \max_{1 \leq i \leq N} (F_a(y_i) - F_b(y_i)) \quad (27)$$

where D is the statistical distance, $F(y)$ is the Cumulative Density Function (CDF) and N is the number of samples. If D is greater than the significance level α then we can reject our null hypothesis. For our problem, after some preliminary tests we set the significance level $\alpha = 0.18$. We set the value higher than the general value of 0.05 because the TH preference of occupants will always have some overlap. Thus discovering a new distribution is defined as:

$$\alpha \leq 0.18 \iff \text{Different Human Model} \quad (28)$$

Using the above equations, we compare the similarity between the current occupant TH embedding and the embeddings stored in the pool. If the similarity is lower than α , we add the embedding in the pool as a new occupant.

5 Experiments and Results

In this section, we present our results using both the proposed POSHS and the baseline LSTM. In the first experiment, we evaluate the POSHS performance by its accuracy in approximating the occupant's distribution accurately in the environment. In the second experiment, we evaluate the impact of the SHS on the occupant by measuring the time-steps required by the occupant to set TH with and without the SHS. We further compare those results to the LSTM baseline.

5.1 Experiment A

In this experiment, we measure the performance of the POSHS in identifying occupants while learning the thermal preferences of each user. We train each human model separately for 350 episodes such that each model can complete each activity while also setting the optimal TH. Next, we train the POSHS with the trained occupant for 150 episodes. During the training of the POSHS, a human model is chosen randomly before each episode. Finally, each human model is run with the POSHS for 50 episodes to evaluate the final performance of the system.

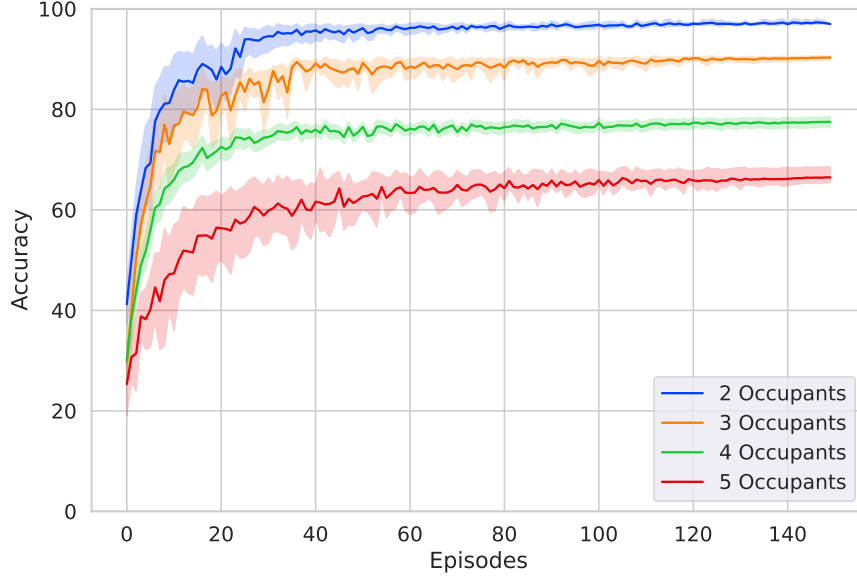


Figure 3: Training accuracy of 2-5 human models with POSHS agent using Jensen-Shannon Divergence to determine distribution similarity.

First, we only experiment with two human models, namely \mathcal{H}_a and \mathcal{H}_b . We set the metabolism indices for \mathcal{H}_a to $[1, 1.2, 1.4]$ based on [3, 21]. For \mathcal{H}_b , slightly different indices are required. We therefore add 0.05 to each of the indices for \mathcal{H}_a to achieve $[1.15, 1.25, 1.45]$ for \mathcal{H}_b for the PMV range of $d_{0.25}$. We use $\tau_{JSD} = 0.13$ which empirically showed the best results in preliminary tests. Figure 3 shows the accuracy of identifying the current model correctly during the training of POSHS. As discussed earlier, the occupant identification is performed by comparing the TH preference distribution estimated by the POSHS from the episode to the ones stored in the pool of distributions using the JSD, and selecting the best match. It can be seen on the Figure 3 that the performance quickly achieves an accuracy of 85% and converges to nearly 100% accuracy.

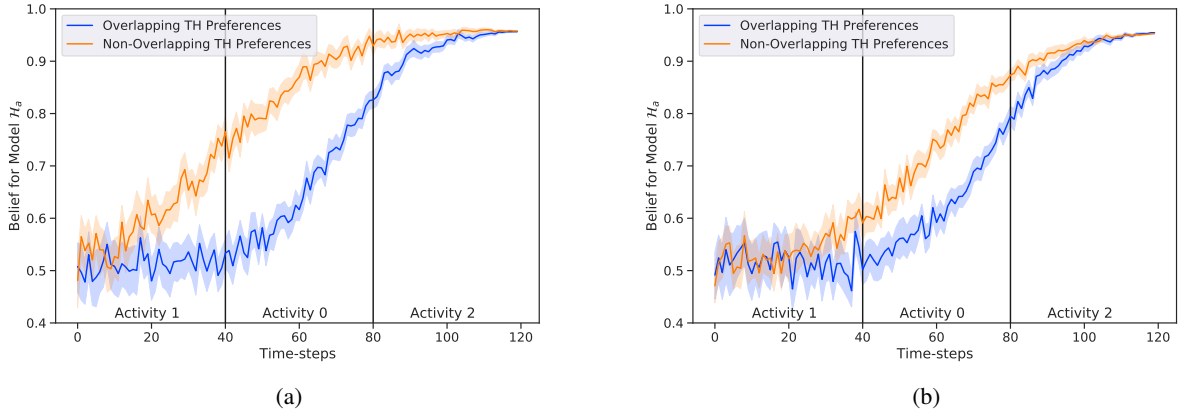


Figure 4: Model \mathcal{H}_a belief update for overlapping ($d_{0.5}$) and non-overlapping ($d_{0.25}$) TH preferences (with Model \mathcal{H}_b). In plot (a), POSHS learns the activity (12D) specific TH distributions of the occupant while in plot (b), it learns the episode (4D) specific TH distribution of the occupant.

To further evaluate the POSHS performance, we repeat the experiment using a wider PMV range of $d_{0.50}$, leading the human models to have more overlapping TH preference distributions. Figure 4(a) shows the average belief of the

POSHS over the occupant during the test episodes. As we can see, when the human model TH preference distributions overlap, it takes more time-steps for the POSHS to properly identify the model’s distribution. To further determine if maintaining the per-activity TH preference distributions (12 dimensional: μ and σ for T and H given each activity) is an important factor in the POSHS’s performances, we repeat the same experiment once more, but using a TH preference distribution that does not encode activity-specific preferences (4 dimensional: μ and σ for T and H for each episode). The results are shown in Figure 4(b). As we can see, compared to Figure 4(a), the two curves are now relatively slow at identifying the current occupant, even when their preference distributions do not overlap as much. For a 12d representation, we re-run preliminary experiments and find $\tau_{JSD} = 0.20$ which empirically showed the best results.

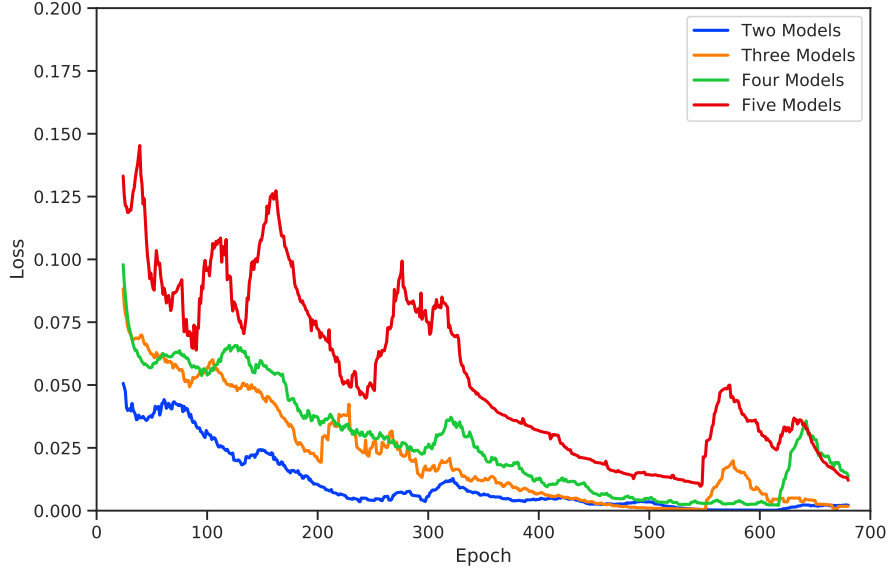


Figure 5: Mean training loss of LSTM with a combination of two, three, four, and five human models in the environment.

Finally, we repeat the same experiment, using 3, 4, and 5 different human models with a PMV range of $d_{0.25}$ (and the 12D TH preference representation). To do so, we increase the indices of \mathcal{H}_a by small fixed amounts to get the metabolism indices for the new human models \mathcal{H}_c , \mathcal{H}_d and \mathcal{H}_E . The final values are $[1.15, 1.22, 1.35]$, $[1.15, 1.25, 1.4]$, and $[1.05, 1.3, 1.45]$, respectively. The final accuracies as well as its test F1 scores are reported in Table 1. We observe that with only two human models, the POSHS is able to perform identification with high accuracy based on the thermal preferences. We also observe that with the integration of more human models, the accuracy drops due to the increased overlap between TH preferences. Nonetheless, strong results (68%) above chance level (20%) are still obtained for higher number of human models, for instance 5.

5.2 Experiment B

Here, we evaluate how both approaches, the POSHS and the LSTM model, perform in terms of rewards and time steps required for the human occupant to set TH as we increase the number of humans models in the home. Note that both POSHS and LSTM must form an internal representation of the underlying hidden state. POSHS does it by explicitly estimating the current occupant’s TH preference, while the LSTM builds an internal representation based on the sequence of observed actions (TH and activities).

Similar to Experiment A, we train the LSTM with the trained human occupant for 175 episodes with a learning rate of 0.0013. During the training, a human model is chosen randomly at the beginning of the episode. We repeat the experiment for up to 5 human models. For testing purposes, we test the LSTM model for 50 episodes to evaluate the final performance. Therefore, both POSHS and LSTM were tested under the same training and testing conditions.

The performance in terms of the occupant’s rewards for both SHS models are shown in Table 2. There is only a slight decrease in the observed mean reward for the occupants with the SHS in comparison to mean reward without the SHS, suggesting that the human occupants spend less time changing the TH in the presence of the SHS model. We then measure the actual number of time-steps required by the occupants to set their preferences with the SHS models

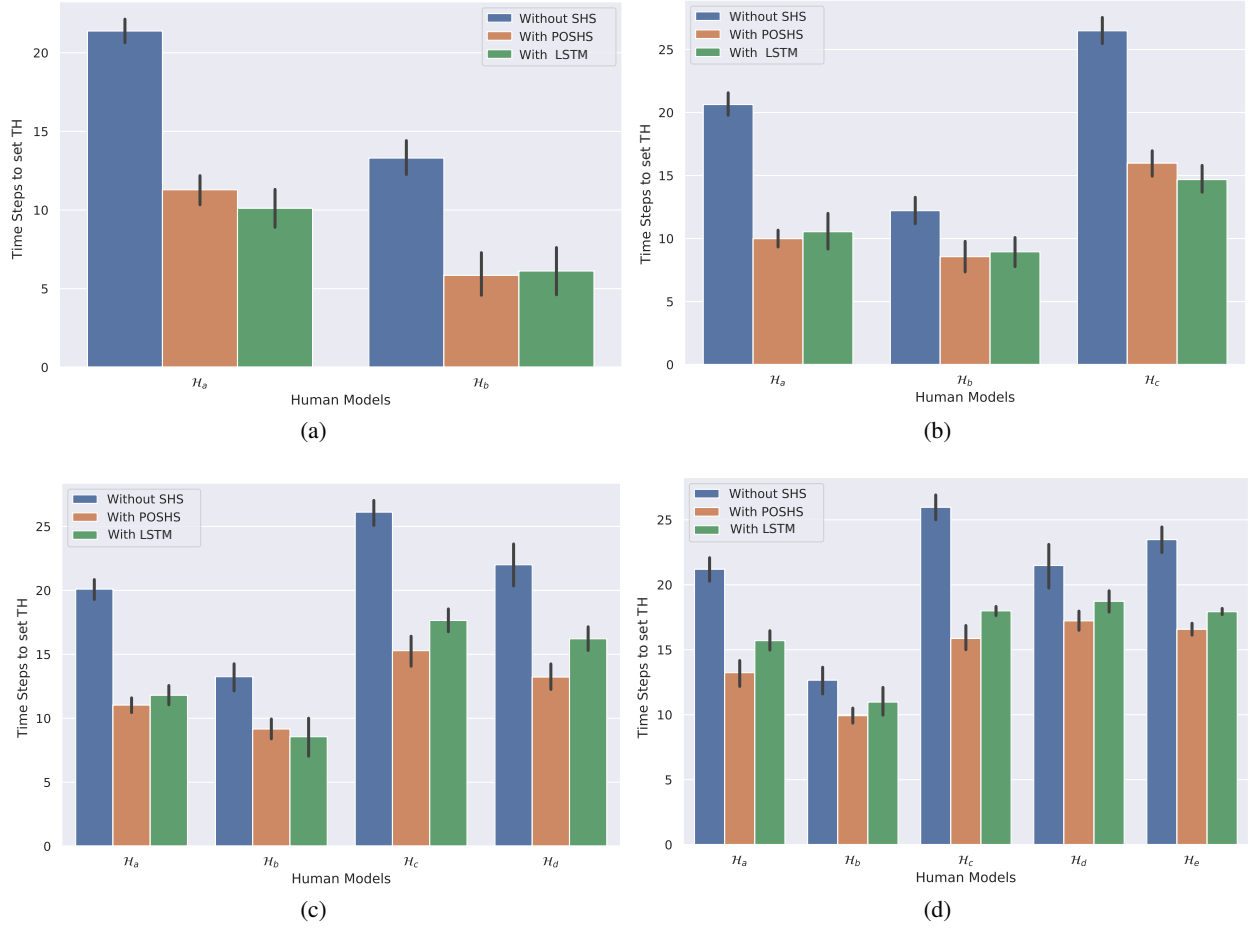


Figure 6: Mean time-steps taken to set TH without SHS, with POSHS, with LSTM for a)two, b)three, c)four, and d)five human models in the environment is shown here. (Lower is better)

compared to the time-steps required by the occupants without the SHS. This is shown in Figure 6 where we present the results for 2, 3, 4, and 5 human occupants in the SHS. It is observed that the number of extra time steps taken by the occupants are close for POSHS and LSTM for up to 3 occupants. However, in Figure 6(c) and (d), that the difference increases substantially with more human occupants for LSTM.

Furthermore, Table 2 shows that POSHS slightly outperform LSTM in the amount of rewards received by the occupant. This difference increases as the number of different human models increases. As shown in Figure 6(a) and (b),

This time-step variation can be observed in Figure ?? is confirmed by the number of time steps the occupants are spending changing temperature in Figure 6 where with the number of time-steps increases with the number of occupants.

A look at the LSTM learning curve (loss during training) further shows that LSTM has much more difficulties learning the Q -values accurately as the number of occupants increases. Those difficulties are highlighted with 5 humans models where LSTM seems to suffer from catastrophic forgetting (peaks in loss curve). This suggest that some mix of training episodes, or some updated in target network, may force the LSTM to changes its internal representation as it trains, to fix its and inappropriate internal representation. But it is commonly very difficult to interpret neural network internal representations [ref]. We can still see that at the end of training, the loss for 4 and 5 occupants is higher than for 2 and 3 occupants.

5.3 Conclusion

In this paper, we investigate the scenario where limited information about the occupants is available to the smart home, resulting is often sub-optimal actions by the smart home in a given state. We model a smart home to learn to recognize

Table 1: POSHS mean Accuracy (in %) and F1 Score for accurately approximating the occupant distribution up to 5 human models.

	Model	POSHS		LSTM	
		Accuracy	F1 Score	Accuracy	F1 Score
2 Models	Model \mathcal{H}_a	0.96	0.98	0.96	0.94
	Model \mathcal{H}_b	1.00	0.98	0.93	0.94
	Mean	0.98	0.96	0.94	0.94
3 Models	Model \mathcal{H}_a	0.92	0.89	0.94	0.93
	Model \mathcal{H}_b	0.96	0.94	0.83	0.84
	Model \mathcal{H}_c	0.92	0.88	0.94	0.88
	Mean	0.90	0.90	0.88	0.88
4 Models	Model \mathcal{H}_a	0.60	0.67	0.60	0.67
	Model \mathcal{H}_b	0.83	0.83	0.64	0.67
	Model \mathcal{H}_c	0.90	0.78	0.89	0.76
	Model \mathcal{H}_d	0.77	0.77	0.75	0.72
	Mean	0.76	0.76	0.70	0.71
5 Models	Model \mathcal{H}_a	0.67	0.63	0.78	0.74
	Model \mathcal{H}_b	0.60	0.60	0.50	0.55
	Model \mathcal{H}_c	0.88	0.78	0.75	0.67
	Model \mathcal{H}_d	0.70	0.70	0.56	0.50
	Model \mathcal{H}_e	0.62	0.70	0.62	0.70
	Mean	0.67	0.68	0.62	0.63

Table 2: Mean Reward values for up to 5 human models for the POSHS and LSTM baseline in comparison to when the SHS is not integrated (higher values are better).

Model	Without SHS	POSHS	LSTM
2 Models	284 \pm 1.17	291 \pm 1.14	290 \pm 1.62
3 Models	283 \pm 1.80	291 \pm 1.81	286 \pm 2.78
4 Models	283 \pm 1.92	287 \pm 3.49	284 \pm 3.89
5 Models	283 \pm 2.35	286 \pm 4.30	283 \pm 5.70

the occupant’s thermal preference distributions using Bayesian modelling, which helps maintain a belief over the hidden user state that the smart home uses to improve its policy. As a baseline for comparison, we design an approach in which the temporal relations between the TH sequences are learned to approximate the hidden state. We integrate both smart home models with up to 5 human models and evaluate them based on their ability to identify the underlying state (or occupant’s TH preferences), as well as the overall human performance in terms of human rewards and time steps spent changing the TH with the SHS. Finally, we compare the POSHS with the baseline model that aims to learn its own representation of underlying states of the partially observable environment. Our simulations show good performance with POSHS when the number of human occupants are low without an increase in time required to set the thermal preferences by the occupant. Similar performance was observed with the baseline. With more human models integrated in the environment, the time-step difference between the baseline and POSHS increases where the occupants now take more time to set the TH with the baseline compared to the POSHS model. In the end, With our simulated experiments, we demonstrate that in an environment where the user information is not fully observable it is possible to approximate the user’s hidden state with multiple occupants without having an impact on the user’s behavior even with sub-optimal approximations.

For future work, our algorithm’s accuracy in approximation of the occupant state can be improved by including other bio-parameters. These parameters can be heart rate, skin temperature, skin sensation, surrounding radiation etc. Some of the most common parameters like heart rate, EC, EEG can be easily obtained from smart watches that is used in vast number by the population. This will not only improve our algorithm’s accuracy but having more data to work with will also enable evaluation of our algorithm for more than 5 humans. Lastly, our algorithm solves the issue of learning the preference of new user without going through any offline training. Another feature that can be implemented to improve online learning of our algorithm is transfer learning from huge amounts of thermal data that is available from other research works thereby reducing the learning time for each human model.

References

- [1] S. M. Ali, J. C. Augusto, and D. Windridge. A survey of user-centred approaches for smart home transfer learning and new user home automation adaptation. *Applied Artificial Intelligence*, 33(8):747–774, 2019.
- [2] E. Arens, H. Zhang, and C. Huizenga. Partial-and whole-body thermal sensation and comfort—part i: Uniform environmental conditions. *Journal of thermal Biology*, 31(1-2):53–59, 2006.
- [3] S. ASHRAE et al. Standard 55-2010, thermal environmental conditions for human occupancy. *American Society of Heating, Refrigerating and Air Conditioning Engineers*, 2010.
- [4] D. M. Endres and J. E. Schindelin. A new metric for probability distributions. *IEEE Transactions on Information theory*, 49(7):1858–1860, 2003.
- [5] A. A. Farhan, K. Pattipati, B. Wang, and P. Luh. Predicting individual thermal comfort using machine learning algorithms. In *2015 IEEE International Conference on Automation Science and Engineering (CASE)*, pages 708–713. IEEE, 2015.
- [6] M. Hausknecht and P. Stone. Deep recurrent q-learning for partially observable mdps. In *2015 aaai fall symposium series*, 2015.
- [7] W. Jung, F. Jazizadeh, and T. E. Diller. Heat flux sensing for machine-learning-based personal thermal comfort modeling. *Sensors*, 19(17):3691, 2019.
- [8] K. Katić, R. Li, and W. Zeiler. Machine learning algorithms applied to a prediction of personal overall thermal comfort using skin temperatures and occupants’ heating behavior. *Applied ergonomics*, 85:103078, 2020.
- [9] J. Kim, Y. Zhou, S. Schiavon, P. Raftery, and G. Brager. Personal comfort models: Predicting individuals’ thermal preference using occupant heating and cooling behavior and machine learning. *Building and Environment*, 129:96–106, 2018.
- [10] D. P. Kingma and J. Ba. Adam: A method for stochastic optimization. *arXiv preprint arXiv:1412.6980*, 2014.
- [11] E. Laftchiev and D. Nikovski. An iot system to estimate personal thermal comfort. In *2016 IEEE 3rd World Forum on Internet of Things (WF-IoT)*, pages 672–677. IEEE, 2016.
- [12] J. Lin. Divergence measures based on the shannon entropy. *IEEE Transactions on Information theory*, 37(1):145–151, 1991.
- [13] S. Liu. Personal thermal comfort models based on physiological parameters measured by wearable sensors. 2018.
- [14] F. J. Massey Jr. The kolmogorov-smirnov test for goodness of fit. *Journal of the American statistical Association*, 46(253):68–78, 1951.
- [15] S. Ross, B. Chaib-draa, and J. Pineau. Bayes-adaptive pomdps. In *NIPS*, pages 1225–1232, 2007.
- [16] S. Ross, J. Pineau, B. Chaib-draa, and P. Kreitmann. A bayesian approach for learning and planning in partially observable markov decision processes. *Journal of Machine Learning Research*, 12(5), 2011.
- [17] F. Salamone, L. Belussi, C. Currò, L. Danza, M. Ghellere, G. Guazzi, B. Lenzi, V. Megale, and I. Meroni. Application of iot and machine learning techniques for the assessment of thermal comfort perception. *Energy Procedia*, 148:798–805, 2018.
- [18] A. K. Sikder, L. Babun, Z. B. Celik, A. Acar, H. Aksu, P. McDaniel, E. Kirda, and A. S. Uluagac. Kratos: Multi-user multi-device-aware access control system for the smart home. In *Proceedings of the 13th ACM Conference on Security and Privacy in Wireless and Mobile Networks*, pages 1–12, 2020.
- [19] R. Sturgeon and F. Rivest. Automatic policy decomposition through abstract state space dynamic specialization. In *2020 International Joint Conference on Neural Networks (IJCNN)*, pages 1–7. IEEE, 2020.
- [20] S. Suman, A. Etemad, and F. Rivest. Potential impacts of smart homes on human behavior: A reinforcement learning approach. *IEEE Transactions on Artificial Intelligence*, pages 1–1, 2021.
- [21] F. Tartarini, S. Schiavon, T. Cheung, and T. Hoyt. Cbe thermal comfort tool: Online tool for thermal comfort calculations and visualizations. *SoftwareX*, 12:100563, 2020.
- [22] Z. Wang, R. de Dear, M. Luo, B. Lin, Y. He, A. Ghahramani, and Y. Zhu. Individual difference in thermal comfort: A literature review. *Building and Environment*, 138:181–193, 2018.
- [23] Z. Wang, T. Parkinson, P. Li, B. Lin, and T. Hong. The squeaky wheel: Machine learning for anomaly detection in subjective thermal comfort votes. *Building and Environment*, 151:219–227, 2019.
- [24] G. M. Weiss, J. L. Timko, C. M. Gallagher, K. Yoneda, and A. J. Schreiber. Smartwatch-based activity recognition: A machine learning approach. In *2016 IEEE-EMBS International Conference on Biomedical and Health Informatics (BHI)*, pages 426–429. IEEE, 2016.
- [25] A. Youssef, A. Youssef Ali Amer, N. Caballero, and J.-M. Aerts. Towards online personalized-monitoring of human thermal sensation using machine learning approach. *Applied Sciences*, 9(16):3303, 2019.
- [26] P. Zhu, X. Li, P. Poupart, and G. Miao. On improving deep reinforcement learning for pomdps. *arXiv preprint arXiv:1704.07978*, 2017.